Oxidation of ethylene by a multistage corona discharge system in the absence and presence of Pt/TiO$_2$

Sumaeth Chavadej [a,*], Kanokwan Saktrakool [a], Pramoch Rangsunvigit [a],
Lance L. Lobban [b], Thammanoon Sreethawong [a]

[a] *The Petroleum and Petrochemical College, Chulalongkorn University, Soi Chula 12, Phyathai Road, Pathumwan, Bangkok 10330, Thailand*
[b] *School of Chemical, Biological, and Materials Engineering, University of Oklahoma, Norman, Oklahoma 73019, USA*

Abstract

The main objective of this work was to investigate a combined plasma and catalytic reactor system for ethylene removal. A four-stage plasma system with wire and plate electrodes was employed to oxidize ethylene as a model pollutant under excess oxygen conditions. The effects of commercial TiO$_2$, sol–gel TiO$_2$, and 1% Pt/sol–gel TiO$_2$ loaded on glass wool used as catalysts packed in the plasma reactors were studied. For the plasma system without a catalyst, both the ethylene conversion and the CO$_2$ selectivity were found to increase with increasing applied voltage and the stage number of the plasma system; but increasing the frequency and feed flow rate gave the opposite effects. The presence of all studied catalysts in the plasma system was found to increase both C$_2$H$_4$ and O$_2$ conversions. The CO$_2$ selectivity increased under the presence of the catalysts in the following order: 1% Pt/sol–gel TiO$_2$ > sol–gel TiO$_2$ = commercial TiO$_2$. When the TiO$_2$ was present in the plasma reactor system, it enhanced the ethylene oxidation reaction because its reducible property provides both the reaction sites and oxygen for the reaction. The presence of 1% Pt on the sol–gel TiO$_2$ was found experimentally to promote the CO oxidation, leading to a higher CO$_2$ selectivity.

1. Introduction

The emission of volatile organic compounds (VOCs) is one of the major sources of air pollution [1]. Air pollutants can enter to the human body mainly by inhalation. Their toxic effect on human health can cause premature death, respiratory illness, alterations in the lung's defenses, and aggravation of existing cardiovascular disease. Furthermore, VOCs are the precursors of smog, ozone, and acidic precipitation (acid rain), and they can affect both terrestrial and aquatic ecosystems, and global warming [2]. Emissions of VOCs come from several vehicular sources and industrial processes, including the chemical industry and petroleum refineries.

There are various methods available for VOC removal, such as liquid absorption, solid adsorption, scrubbing, condensation, biodegradation, thermal incineration, and catalytic combustion [3]. Combustion is the most effective way to achieve complete destruction of VOCs, but the energy requirement for complete combustion is rather high. Non-thermal plasma and photocatalytic processes have been considered as promising alternatives for the economical removal of VOCs since they can operate at ambient conditions. Recently, much attention has also been focused on the combined use of non-thermal plasma and catalytic/photocatalytic processes for VOC removal [4–10]. Moreover, in the presence of excess oxygen, the main products from these processes are carbon dioxide and water.

For non-thermal plasma, a high voltage is applied across two metal electrodes to produce high-energy electrons that can directly initiate the oxidative reaction to decompose organic pollutants [11]. During plasma generation, active species, radicals, and ions are formed, as well as UV radiation, by the collision of high-energy electrons emitted from the surfaces of electrodes under high voltage [11–13]. Our previous work showed that the degradation of ethylene using a combined plasma and catalytic reactor was greatly affected by the residence time [12].

In a comparison between ac and dc discharges for the oxidative methane reaction, ac discharge was found to be greatly superior to dc discharge [14]. As ac discharge is applied, each

* Corresponding author. Tel.: +66 2 218 4139; fax: +66 2 218 4139.
  E-mail address: sumaeth.c@chula.ac.th (S. Chavadej).

electrode performs alternatively as an anode and cathode. The space charge between the two electrodes is eliminated and then a new space charge is initiated every half cycle. With increasing frequency, a faster reversal of the electric field reduces the decay of the space charge. Acceleration of the remaining space charge by the reversing electric field can decrease the amount of current required to sustain the discharge. Therefore, the ac plasma was selected for this present study.

In this work, a four-stage plasma reactor system was used to investigate oxidation of ethylene, which was selected as a representative of hydrocarbon pollutants. The effect of TiO_2 and Pt/TiO_2 used as catalysts in the plasma reactors on the ethylene removal was also studied.

2. Experimental

2.1. Materials

Platinum(II)2,4-pentanedionate, $Pt(C_5H_7O_2)_2$, obtained from Alfa Aesar, and tetraethylorthotitanate (TEOT), supplied by Fluka, were used as precursors for preparing platinum and titania (TiO_2), respectively. The activity of the catalysts prepared by the sol–gel method was compared with commercially available titania dioxide obtained from J.J. Degussa Hüls (T) Co. Ltd (Degussa P25). All chemicals were used as received without further purification.

2.2. Catalyst preparation

In order to prepare the commercial TiO_2 coated on glass wool, a sheet of glass wool (3 cm × 3 cm) was first dipped into a solution of 2% commercial TiO_2 in distilled water. Afterwards, the coated glass wool was dried at 100 °C for 10 min, followed by calcination at 300 °C for 3 h. For preparing the sol–gel TiO_2 coated on glass wool, 1.5 g of tetraethylorthotitanate (TEOT) was mixed with 20 ml of ethanol and six drops of nitric acid to form a gel solution. A sheet of glass wool was then dipped into the gel solution. The coated glass wool was dried at 100 °C for 10 min and then calcined at 400 °C for 5 h. To prepare 1% Pt/sol–gel TiO_2, 0.005 g of $Pt(C_5H_7O_2)$ and 2.83 g of TEOT were dissolved in 38.07 ml of ethanol and 14 drops of nitric acid. The same coating procedure was carried out as described before.

2.3. Catalyst characterization

The specific surface areas of the prepared catalysts were measured with a Quantachrom surface area analyzer (Autosorb-1) using nitrogen adsorption analysis. Crystalline phases of the prepared catalysts were determined by a Rigaku X-ray diffractometer (RINT-2200) equipped with a graphite monochromator and a Cu tube for generating Cu Kα radiation ($\lambda = 1.5406$ Å) at a generator voltage and current of 40 kV and 30 mA, respectively. A nickel filter was used as the Kα filter. The goniometer parameters were divergence slit = 1° (2θ), scattering slit = 1° (2θ), and receiving slit = 0.3 mm. The catalyst sample was held on a glass slide holder and was examined between 5° and 90° (2θ) range
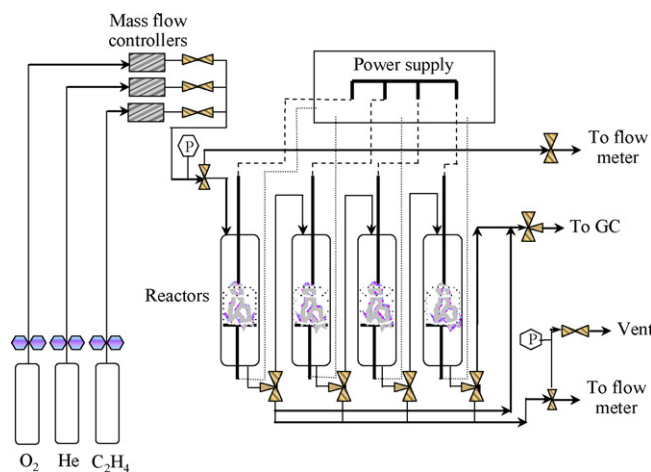

Fig. 1. Schematic of the experimental set-up.

at a scanning speed of 5° (2θ)/min and a scan step of 0.02° (2θ). The surface morphology of all prepared catalysts was examined by using a scanning electron microscope (JEOL, JM-5200).

2.4. Experimental setup and oxidation experiments

A schematic of the experimental setup in this work is shown in Fig. 1. A feed gas was prepared by the mixing of three reactant gases: 99.99% ethylene, 99.5% oxygen, and 99.95% helium. The flow rates of these three reactant gases were controlled by mass flow controllers to obtain 3% ethylene and 15% oxygen with helium balance, which provides 67% excess oxygen based on the complete oxidation reaction of ethylene. The high concentration of 3% ethylene was selected in this study because all product gases can be easily detected. Helium was used as a dilution gas in order to avoid any complication from the formation of nitrogen oxides if air is used instead. Before the reactant gases passed through the mass flow controllers, any foreign particles in the reactant gases were trapped using 0.7 μm in-line filters. The reactors were made of quartz tubes with a 10 mm outside diameter and an 8 mm inside diameter. The plasma reactors were operated under atmospheric pressure, and the feed gas temperature was around 25–27 °C (room temperature). Plasma was generated in each reactor across a stainless steel wire electrode and a plate electrode with a gap distance of 1 cm. The power used to generate plasma was alternating current at 220 V and 50 Hz, which was transmitted to a high voltage side. The output voltage was increased to 130 times its original voltage, and the signal of the alternating current was a sinusoidal form. It was not possible to directly measure the voltage across the electrodes of the reactor (high-side voltage). Therefore, the low-side voltage and current were measured instead, and the high-side voltage and current were then calculated by multiplying and dividing by a factor of 130, respectively.

After the feed mixture gas was introduced into the plasma system for about 30 min, the power supply unit was turned on. In this experiment, the feed gas flow rate, applied voltage, and frequency were varied. After the studied system was allowed to run for 30 min, the composition of the effluent was analyzed every 30 min until the outlet gas composition was constant, indicating

the plasma system reached steady state. The effects of the stage number of the plasma system on the ethylene removal and product selectivities were investigated by varying one to four reactors in series, which was done by turning off the power supply one by one. The compositions of both feed gas and effluent gas were analyzed by using an on-line GC (Perkin-Elmer, AutoSystem GC) equipped with a packed column (Carboxen 1000) and a thermal conductivity detector. The experimental data taken under steady state conditions were averaged, and these averages were used to evaluate the performance of the plasma system.

To investigate the effects of catalyst in the plasma reactors on the ethylene decomposition, the sol–gel TiO_2 or 1% Pt/sol–gel TiO_2 coated on glass wool was packed in the space between the two electrodes. In addition, the commercial TiO_2 was also tested for comparisons.

Under the studied conditions, CO, CO_2, and H_2O were found as the reaction products with trace amounts of other intermediate products (methane, ethane, and acetylene). The temperature of the outlet gas downstream of the plasma zone was in the range of 150–200 °C. To evaluate the process performance of the plasma system, the conversions of ethylene and oxygen and the selectivities of CO and CO_2 were used. The conversion of either ethylene or oxygen is defined as

%reactant conversion

$$= \frac{(\text{mole of reactant } in - \text{mole of reactant } out) \times 100}{\text{mole of reactant } in} \quad (1)$$

The product selectivity (CO or CO_2) is calculated from the following equation:

$$\%\text{product selectivity} = \frac{[(\text{number of carbon atom in product})(\text{mole of product produced})] \times 100}{(\text{number of carbon atom in ethylene})(\text{mole of ethylene converted})} \quad (2)$$

To determine the energy efficiency of the plasma system, the specific energy consumption is calculated in a unit of electron-Volt per one molecule of ethylene converted as the following equation:

specific energy consumption $(eV/mol\ C_2H_4)$

$$= \frac{(60)(P)}{(1.602 \times 10^{-19})NM_c} \quad (3)$$

where P is the input power (W), N is the Avogadro's number = 6.02×10^{23} molecules/g mol, M_c is the rate of ethylene in feed converted (g mol/min) and $1\ eV = 1.602 \times 10^{-19}$ W s.
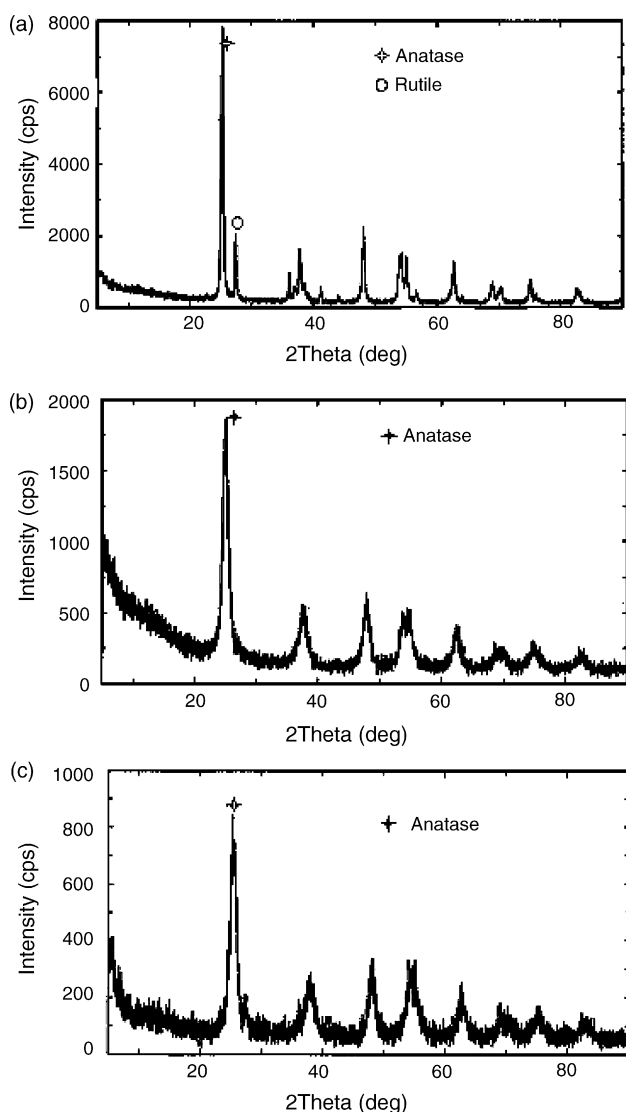
3. Results and discussion

3.1. Catalyst characteristics

The measured values of BET specific surface areas of the commercial TiO_2, sol–gel TiO_2, and 1% Pt/sol–gel TiO_2 are 63.77, 103.1, and 103.5 m^2/g, respectively. The crystal structures of the studied catalysts, which were identified by XRD patterns, are shown comparatively in Fig. 2. All catalysts show the anatase peaks observed prominently at the same position of 2θ, whereas the rutile peak was only observed for the commercial TiO_2. It is worth noting that no peaks of platinum at $2\theta = 40°$ and $48°$ were observed, suggesting that Pt was highly dispersed on all TiO_2 catalysts. The XRD results indicate that the commercial TiO_2 is more crystalline than both sol–gel TiO_2 catalysts. The sol–gel TiO_2 catalysts do not have the rutile peak since the sol–gel TiO_2 catalysts were calcined at a low temperature of 400 °C. The surface morphology of the studied catalysts coated on glass wool was also examined by using SEM analysis. Fig. 3 shows the topography of the commercial TiO_2, sol–gel TiO_2, and 1% Pt/sol–gel TiO_2 coated on glass wool. According to the SEM images, the surface characteristics of both sol–gel TiO_2 and 1% Pt/sol–gel TiO_2 coated on glass wool are much smoother than that of the commercial TiO_2.
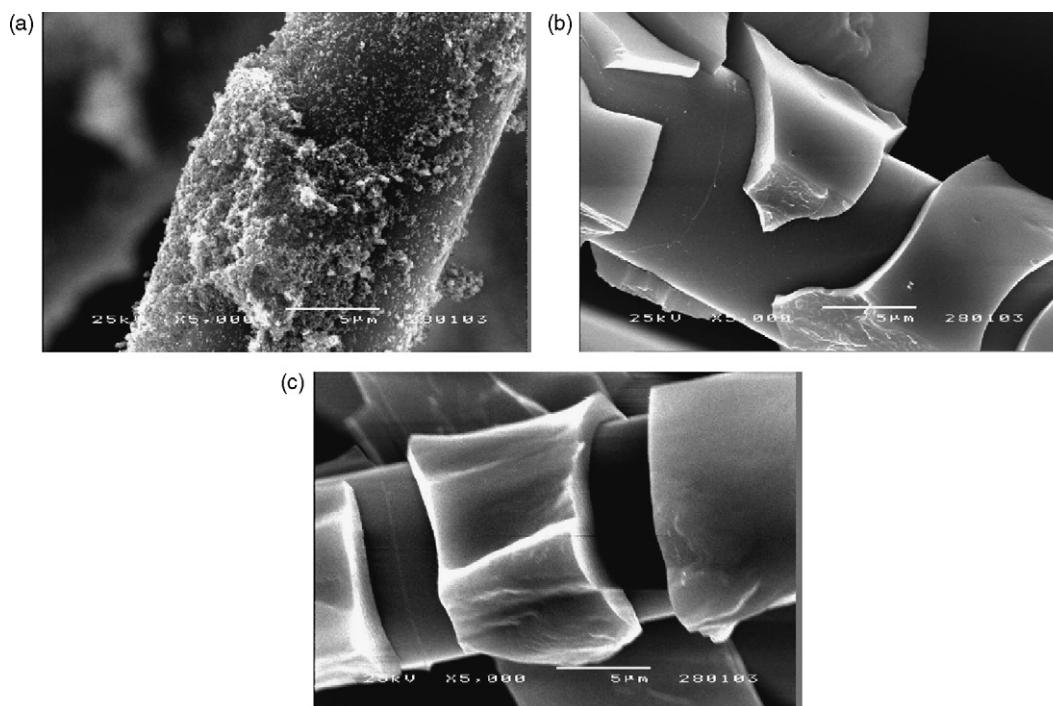

Fig. 2. XRD patterns of (a) commercial TiO_2, (b) sol–gel TiO_2, and (c) 1% Pt/sol–gel TiO_2.

Fig. 3. SEM images of (a) commercial TiO_2, (b) sol–gel TiO_2, (c) 1% Pt/sol–gel TiO_2 coated on glass wool (bar = 5 μm).

3.2. Effect of frequency

The studied plasma system was operated in the 50–700 Hz frequency range since a large amount of coke was found to deposit on the electrode surface at a frequency lower than 50 Hz, and the plasma could not exist at a frequency higher than 700 Hz. Fig. 4(a) illustrates the effects of frequency on the C_2H_4 and O_2 conversions. The conversions of both C_2H_4 and O_2 decreased with increasing frequency in the range of 50–700 Hz. The explanation is that a higher frequency results in a lower current that corresponds to the reduction of the number of electrons generated [13], as confirmed by Fig. 5. The more electrons generated, the higher the opportunity of collision between electrons and O_2 and C_2H_4 molecules. As a result, both conversions of C_2H_4 and O_2 increase with decreasing frequency. For any given frequency, the conversions of C_2H_4 and O_2 increased with increasing the stage number of the plasma reactors since the residence time is increased.

The effects of frequency on the CO and CO_2 selectivities are shown in Fig. 4(b). When the frequency increased, the CO_2 selectivity decreased, whereas the CO selectivity increased. As mentioned before, at a lower frequency, a larger number of electrons are generated from the electrodes, leading to more active oxygen species being produced. As a result, the CO produced is further oxidized to CO_2. For any given frequency, the CO_2 selectivity also increased, while the CO selectivity decreased with increasing stage number of the plasma reactors because the electrons have more chances to break down O_2 to produce the active oxygen species.

The effect of frequency on the power consumption to break down each C_2H_4 molecule is shown in Fig. 6. Interestingly, the minimum power was found to be in the frequency range

of 200–500 Hz. At a frequency lower than the optimum range, a larger number of electrons are generated, leading to higher power consumption, as verified by Fig. 5. On the other hand, a higher frequency corresponds to a reduced number of generated electrons, leading to reducing C_2H_4 decomposition. To obtain the minimum power consumption, as well as to have a relatively high C_2H_4 conversion, a frequency of 200 Hz was selected for further experiments.

3.3. Effect of applied voltage

Under the studied conditions, the break-down voltage or the lowest voltage (onset voltage) to generate plasma was found to be about 9000 V, and the complete conversion of ethylene occurred at 15,000 V with the four-stage system. Hence, the reaction experiments were conducted in the voltage range of 9000–15,000 V in order to determine the effect of the applied voltage. Fig. 7(a) shows the effects of applied voltage on the C_2H_4 and O_2 conversions. The conversions of C_2H_4 and O_2 increased slightly with increasing applied voltage, which is in contrast with the effect of frequency. The explanation is that a higher voltage results in increasing electric field strength [15], as also confirmed by Fig. 8, promoting a larger number of electrons with high energy, which, in turn, increases the conversions. An increase in the stage number of the plasma reactors resulted in increasing both conversions of ethylene and oxygen since the system has a longer residence time, leading to electrons having more chance to break down C_2H_4 and O_2 molecules.

The effects of applied voltage on the selectivities of CO and CO_2 are shown in Fig. 7(b). As the applied voltage increased, the CO_2 selectivity increased, whereas the CO selectivity decreased. This is because an increase in voltage results in increasing cur-
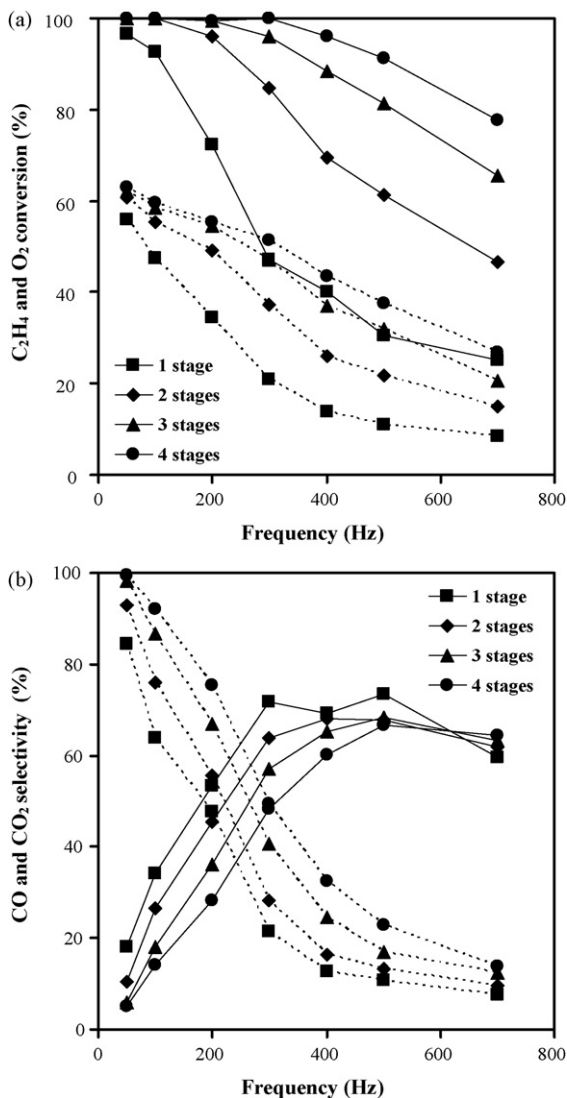
(a)

(b)

Fig. 4. Effects of frequency (a) on C_2H_4 and O_2 conversions (solid line: C_2H_4 conversion; dotted line: O_2 conversion) and (b) on CO and CO_2 selectivities (solid line: CO selectivity; dotted line: CO_2 selectivity) (flow rate = 160 ml/min; applied voltage = 11,000 V; gap distance = 1 cm; residence time for 1, 2, 3, and 4 stages = 0.19, 0.38, 0.57, and 0.75 s, respectively).

rent across the electrodes, as shown in Fig. 8. As a result, there are more active oxygen species available to oxidize CO molecules, leading to a higher CO_2 selectivity. For any given applied voltage, the CO selectivity decreased, while the CO_2 selectivity increased when the gas mixture was passed through a higher stage number of the plasma system. The reason is that a higher stage number of the plasma system simply has a longer residence time, leading to enhancing the CO oxidation reaction.

3.4. Effect of feed flow rate

Fig. 9(a) illustrates the effects of feed flow rate on the C_2H_4 and O_2 conversions. For either the single or two-stage system, both C_2H_4 and O_2 conversions decreased with increasing feed flow rate in the studied range of feed flow rate because an
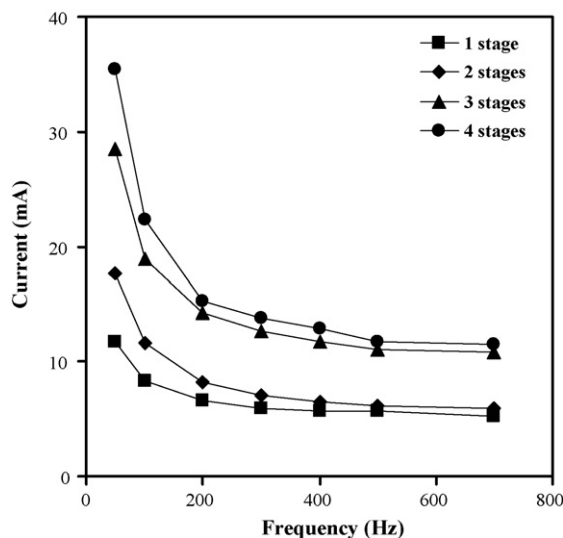

Fig. 5. Effect of frequency on generated current (flow rate = 160 ml/min; applied voltage = 11,000 V; gap distance = 1 cm; residence time for 1, 2, 3, and 4 stages = 0.19, 0.38, 0.57, and 0.75 s, respectively).

increase in the feed flow rate corresponds to a decrease in the residence time. With an increase in the feed flow rate (resulting in lower residence time), electrons have less possibility to collide with C_2H_4 and O_2 molecules, leading to decreasing the conversions of both reactants. Based on the results, the plasma system having three or four stages gave the complete removal of C_2H_4 under an applied voltage of 11,000 V and a frequency of 200 Hz.

The effects of feed flow rate on the CO and CO_2 selectivities are shown in Fig. 9(b). For any given number of stages, the CO selectivity increased with increasing the feed flow rate, while the opposite trend was found for the CO_2 selectivity. A higher feed flow rate reduces the opportunity of collision between electrons and O_2 and C_2H_4 molecules because of the lowering of residence
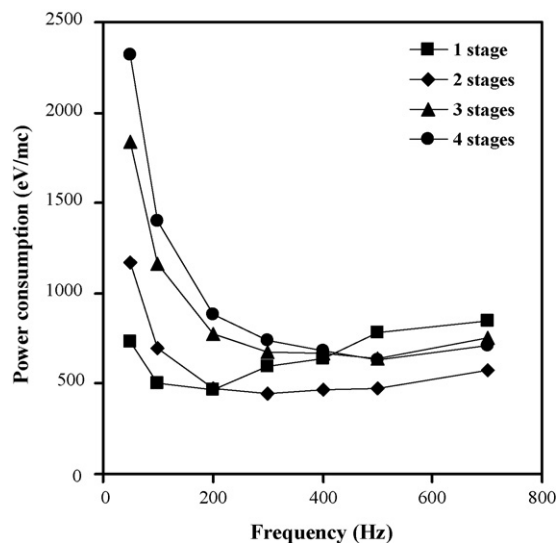

Fig. 6. Effect of frequency on power consumed to convert an ethylene molecule (flow rate = 160 ml/min; applied voltage = 11,000 V; gap distance = 1 cm; residence time for 1, 2, 3, and 4 stages = 0.19, 0.38, 0.57, and 0.75 s, respectively).
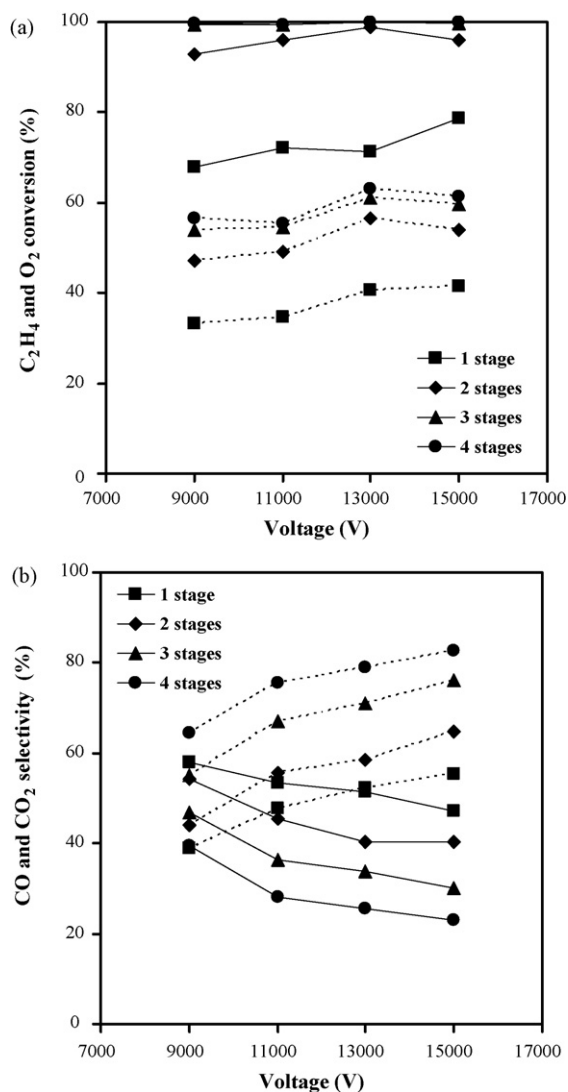
Fig. 7. Effects of applied voltage (a) on C_2H_4 and O_2 conversions (solid line: C_2H_4 conversion; dotted line: O_2 conversion) and (b) on CO and CO_2 selectivities (solid line: CO selectivity; dotted line: CO_2 selectivity) (flow rate = 160 ml/min; frequency = 200 Hz; gap distance = 1 cm; residence time for 1, 2, 3, and 4 stages = 0.19, 0.38, 0.57, and 0.75 s, respectively).

time. Therefore, the oxidation of CO is reduced, resulting in lower CO_2 formation.

3.5. Effect of stage number

To determine the effect of the stage number of the plasma system, the total residence time of the feed gas in the plasma reactors had to be kept constant while the stage number of the reactors was varied. In this study, the residence time is calculated based on the reaction volume between the two electrodes. Fig. 10(a) shows the effects of stage number of the plasma system on the C_2H_4 and O_2 conversions. Under the studied conditions, complete conversion of C_2H_4 was observed at a residence time of 0.75 s or higher. It is clearly seen that for the lowest residence time of 0.38 s, the conversion of C_2H_4 increased with increasing number of stages. For a residence time greater than 0.38 s, the effect of the stage number did not appear because the C_2H_4
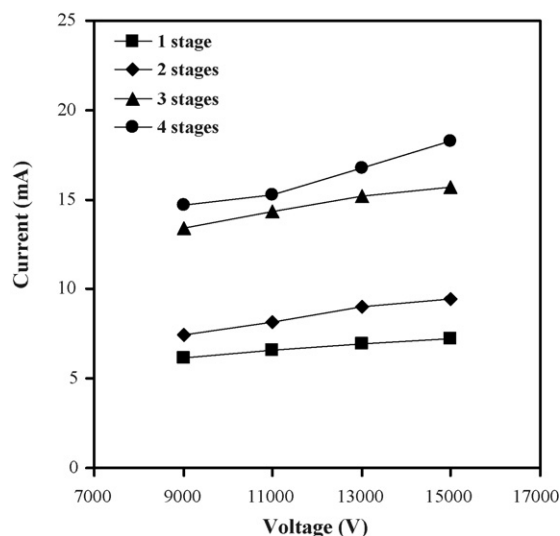

Fig. 8. Effect of applied voltage on generated current (flow rate = 160 ml/min; frequency = 200 Hz; gap distance = 1 cm; residence time for 1, 2, 3, and 4 stages = 0.19, 0.38, 0.57, and 0.75 s, respectively).

conversion almost reached 100%. For any given residence time, an increase in the stage number seems not to affect the oxygen conversion significantly since C_2H_4 was completely removed under the studied conditions.

The effects of stage number on the CO and CO_2 selectivities are shown in Fig. 10(b). As the stage number of the plasma system increased, the CO_2 selectivity increased, whereas the CO selectivity decreased. The explanation is that at a higher stage number, the possibility of the collision between electrons and O_2 molecules is greatly increased. As a result, the oxidation of CO increases, leading to a higher CO_2 selectivity.

3.6. Effect of the presence of catalysts

Table 1 shows the effects of the presence of different catalysts on the conversions of C_2H_4 and O_2 and the product selectivities. It appears that the presence of the commercial TiO_2, sol–gel TiO_2, or 1% Pt/sol–gel TiO_2 significantly increased the C_2H_4 conversion by 20% and 10% with one and two stages in operation, respectively. However, the same effect was not observed when the plasma system having more than two stages was used. This is because the system almost reached the complete conversion of C_2H_4. Both sol–gel TiO_2 and commercial TiO_2 gave similar conversions of O_2 and C_2H_4, indicating that both surface area and crystallinity of TiO_2 play important roles in governing the conversions [16]. For any given stage number, the presence of all studied catalysts appeared to increase the C_2H_4 and O_2 conversions in the following order: 1% Pt/sol–gel TiO_2 > sol–gel TiO_2 ≈ the commercial TiO_2. The reason is that TiO_2 is a reducible oxide and semiconductor in nature. Therefore, it provides the reaction sites and oxygen for the oxidative reaction. In addition, the energy released from the plasma, especially in the form of UV, will excite TiO_2 to create photoinduced species in both the conduction band and the valance band due to the energy band gap excitation, leading to the creation of both oxidation and reduction reactions on the TiO_2 surface. In order to
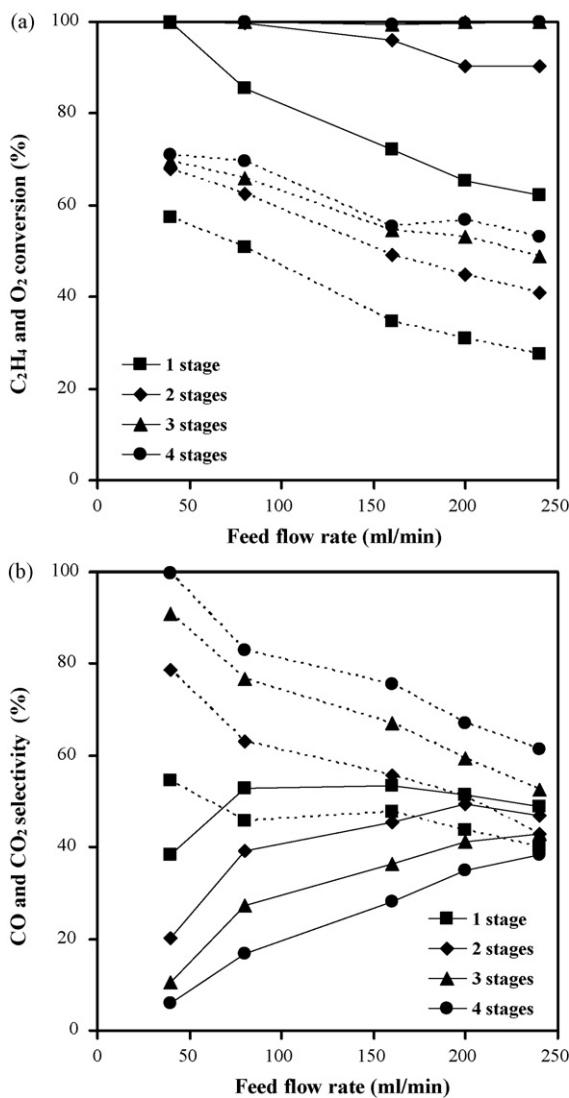
Fig. 9. Effects of feed flow rate (a) on C_2H_4 and O_2 conversions (solid line: C_2H_4 conversion; dotted line: O_2 conversion) and (b) on CO and CO_2 selectivities (solid line: CO selectivity; dotted line: CO_2 selectivity) (frequency = 200 Hz; applied voltage = 11,000 V; gap distance = 1 cm).

Fig. 10. Effects of stage number (a) on C_2H_4 and O_2 conversions (solid line: C_2H_4 conversion; dotted line: O_2 conversion) and (b) on CO and CO_2 selectivities (solid line: CO selectivity; dotted line: CO_2 selectivity) with different residence times (frequency = 200 Hz; applied voltage = 11,000 V; gap distance = 1 cm).

verify the photocatalytic effect of TiO_2, the UV intensity emitted from the plasma generated in the first reactor was measured by using a UV meter. The calculated energy of UV illumination was about 3.39 μW, which is considerably low compared to the input energy of 97 W. It can be concluded that the catalytic property of TiO_2 to provide the reaction site and its reducible property are mainly responsible for the enhancement of the C_2H_4 oxidation reaction, with a minor photocatalytic effect.

The presence of either the sol–gel TiO_2 or commercial TiO_2 increased the CO_2 selectivity by 4–7%, but decreased the CO selectivity by 6%. With 1% Pt loaded on the sol–gel TiO_2, the CO_2 selectivity increased significantly, about 10–17%. Since Pt deposited on TiO_2 plays a significant role in the inhibition of the recombination process of photoinduced species, the acceleration of superoxide radical anion ($O_2^{•-}$) formation is consequently achieved, leading to enhanced photocatalytic activity [17]. In addition, Pt catalyst supported on TiO_2 has
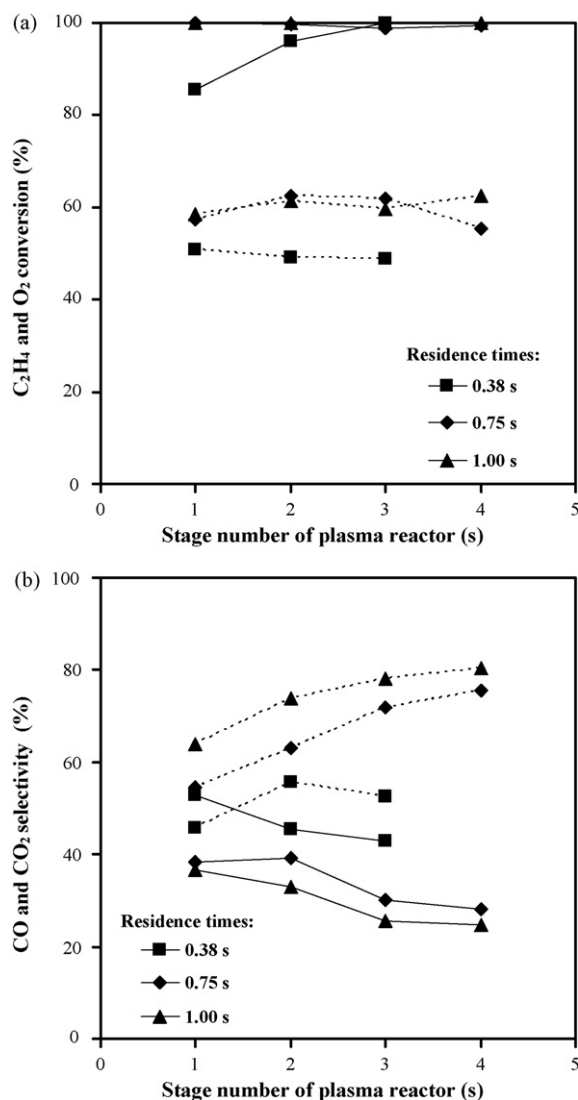
been proven to effectively promote the CO oxidation since it can also stabilize O^- and O_3^- species photogenerated on the TiO_2 surface, which are responsible for the CO oxidation [9,18–20].

The reaction mechanism of ethylene oxidation under the combined catalytic and plasma condition cannot be ruled out based on the present results. However, the possible reactions believed to occur are as follows:

$$e^- + O_2 \rightarrow O^- + O \tag{4}$$

$$C_2H_4 + O^- \rightarrow C_2H_3 + OH^- \tag{5}$$

$$C_2H_3 + 4O \rightarrow 2CO_2 + 3H \tag{6}$$

$$C_2H_3 + O^- \rightarrow C_2H_2 + OH^- \tag{7}$$
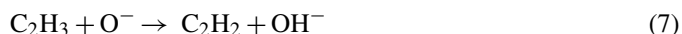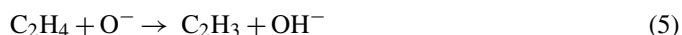
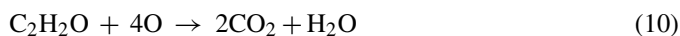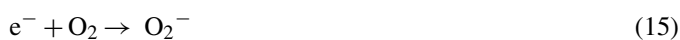$$C_2H_2 + 5O \rightarrow 2CO_2 + H_2O \tag{8}$$

Table 1
Comparative results of the plasma system with and without catalyst (flow rate = 160 ml/min; applied voltage = 9000 V; frequency = 200 Hz; gap distance = 1 cm; catalyst weight = 0.008 g)

Reactor	% conversion		% selectivity	
	C_2H_4	O_2	CO	CO_2
No catalyst				
1st	47	22	70	29
2nd	80	37	61	35
3rd	95	47	52	46
4th	99	52	43	56
Commercial TiO_2				
1st	67	30	58	36
2nd	90	43	56	42
3rd	98	50	48	51
4th	99	53	41	60
TiO_2 (sol–gel)				
1st	68	33	57	38
2nd	90	44	55	43
3rd	99	50	48	51
4th	99	54	41	60
1% Pt/TiO_2 (sol–gel)				
1st	68	35	56	46
2nd	90	46	55	46
3rd	98	53	46	56
4th	99	57	35	70

$$C_2H_2 + O \rightarrow C_2H_2O \tag{9}$$

$$C_2H_2O + 4O \rightarrow 2CO_2 + H_2O \tag{10}$$

$$C_2H_2O + O \rightarrow 2CHO \tag{11}$$

$$2CHO + O \rightarrow H_2 + 2CO \tag{12}$$

$$H_2 + O \rightarrow H_2O \tag{13}$$

$$CO + O \rightarrow CO_2 \tag{14}$$

In the presence of TiO_2:

$$e^- + O_2 \rightarrow O_2^- \tag{15}$$

$$CO + O_2^- \rightarrow CO_2 + O^- \tag{16}$$

It should be mentioned here that the experimental conditions were designed to be able to determine the effects of all process parameters, so the C_2H_4 conversion was below 100%. As known, the complete removal of ethylene without CO formation is needed for real application. Based on the present results, as shown in Table 1, a plasma system should have at least three stages, and it should be operated at a very long residence time (at least a few seconds) to ensure the complete conversion of C_2H_4. The use of 1% Pt/TiO_2 catalyst is strongly recommended to enhance the CO oxidation, leading to the complete oxidation.

4. Conclusions

From the experimental results of the sole plasma system and the plasma system combined with the TiO_2 catalysts, ethylene was almost completely removed by the corona discharge especially with three or four stages. The ethylene removal efficiency decreased with increasing frequency since a higher frequency results in decreased current that corresponds to a reduced number of electrons generated. An increase in feed flow rate decreased the C_2H_4 and O_2 conversions and the CO_2 selectivity as a result of decreasing residence time. The increase in the stage number significantly increased both C_2H_4 conversion and CO_2 selectivity. The presence of catalysts, the commercial TiO_2 or the TiO_2 prepared by the sol–gel method, enhanced both C_2H_4 and O_2 conversion as well as the CO_2 selectivity because TiO_2 is a reducible oxide and provides the reaction sites for the oxidation reactions. It is believed that the UV light liberated from the plasma generation activates TiO_2 to promote the complete oxidation reaction. As expected, the presence of 1% Pt on TiO_2 increased the CO_2 selectivity since the Pt catalyst assists in producing superoxide radical anion, $O_2^{\bullet-}$, and decreasing the recombination process.

Acknowledgments

References

[1] N. De Nevers, Air Pollution Control Engineering International Editions, McGraw-Hill, New York, 1995.
[2] P. Papaethimiou, T. Ioanides, X.E. Verykios, Combustion of non-halogenated volatile organic compounds over group VIII metal catalysts, Appl. Catal. B: Environ. 13 (1997) 175–184.
[3] Y. Cheng, Kinetic and Mechanistic Studies of Volatile Organic Compound Oxidation Catalysis Using Thin Film Model Pt Catalysts, A Research Proposal Submitted in Partial Fulfillment of the Preliminary Examination Requirements, The University of Michigan, 1996.
[4] K. Urashima, J.S. Chang, Removal of volatile organic compounds from air streams and industrial flue gases by non-thermal plasma technology, IEEE Trans. Dielect. El. In. 7 (2000) 602–614.
[5] U. Roland, F. Holzer, F.D. Kopinke, Combination of non-thermal plasma and heterogeneous catalysis for oxidation of volatile organic compounds. Part 2. Ozone decomposition and deactivation of γ-Al₂O₃, Appl. Catal. B: Environ. 58 (2005) 217–226.
[6] U. Roland, F. Holzer, A. Pöppl, F.D. Kopinke, Combination of non-thermal plasma and heterogeneous catalysis for oxidation of volatile organic compounds. Part 3. Electron paramagnetic resonance (EPR) studies of plasma-treated porous alumina, Appl. Catal. B: Environ. 58 (2005) 227–234.
[7] F. Holzer, F.D. Kopinke, U. Roland, Influence of ferroelectric materials and catalysts on the performance of non-thermal plasma (NTP) for the removal of air pollutants, Plasma Chem. Plasma Process. 25 (2005) 595–611.
[8] T. Oda, S.B. Han, R. Ono, Dilute trichloroethylene decomposition in air by the non-thermal plasma process combined with the manganese oxide, J. Adv. Oxid. Technol. 8 (2005) 18–24.

[9] T. Sano, N. Negishi, E. Sakai, S. Matsuzawa, Contribution of photocatalytic/catalytic activities of TiO_2 and in nonthermal plasma on oxidation of acetaldehyde and CO, J. Mol. Catal. A: Chem. 245 (2006) 235–241.

[10] Ch. Subrahmanyam, A. Renken, L. Kiwi-Minsker, Catalytic abatement of volatile organic compounds assisted by non-thermal plasma. Part II. Optimized catalytic electrode and operating conditions, Appl. Catal. B: Environ. 65 (2006) 157–162.

[11] L.A. Rosacha, G.K. Anderson, L.A. Bechtold, J.J. Coogan, H.G. Heck, M. Kang, W.H. McCulla, R.A. Tennant, P.J. Wantuck, Treatment of hazardous organic wastes using silent discharge plasmas, non-thermal plasma technique for pollution control, NATO ASI Ser. 34 (Part B) (1993) 128–139.

[12] B. Harndumrongsak, L.L. Lobban, P. Rangsunvigit, B. Kitiyanan, Oxidation of ethylene in plasma environment, in: Proceedings of the 9th APCChE Congress, Christchurch, New Zealand, September 29–October 3, 2002.

[13] K. Supat, S. Chavadej, L.L. Lobban, R.G. Mallinson, Synthesis gas production from partial oxidation of methane with air in ac electric gas discharge, Energy Fuel 17 (2003) 474–481.

[14] C. Liu, A. Marafee, B. Hill, G. Xu, R.G. Mallinson, L.L. Lobban, Oxidative coupling of methane with ac and dc corona discharge, Ind. Eng. Chem. Res. 35 (1996) 3295–3301.

[15] K. Morinaga, M. Suzuki, The chemical reaction in silent electric discharge. II. The frequency effect on ozone formation, Bull. Chem. Soc. Jpn. 35 (1962) 204–217.

[16] H. Yu, S.C. Lee, J. Yu, C.H. Ao, Photocatalytic activity of dispersed TiO_2 particles deposited on glass fibers, J. Mol. Catal. A: Chem. 246 (2006) 206–211.

[17] A. Blazkova, I. Csolleova, V. Brezova, Effect of light sources on the phenol degradation using Pt/TiO_2 photocatalysts immobilized on glass fibers, J. Photochem. Photobiol. A: Chem. 113 (1998) 251–256.

[18] H. Einaga, A. Ogata, S. Futamura, T. Ibusuki, The stabilization of active oxygen species by Pt supported on TiO_2, Chem. Phys. Lett. 338 (2001) 303–307.

[19] S. Hwang, M.C. Lee, W. Choi, Highly enhanced photocatalytic oxidation of CO on titania deposited with Pt nanoparticles: kinetic and mechanism, Appl. Catal. B: Environ. 46 (2003) 49–63.

[20] J. Yu, J. Xiong, B. Cheng, S. Liu, Fabrication and characterization of $Ag–TiO_2$ multiphase nanocomposite thin films with enhanced photocatalytic activity, Appl. Catal. B: Environ. 60 (2005) 211–221.